Molecular characterization of organic aerosol using nanospray desorption/electrospray ionization mass spectrometry: CalNex 2010 field study

Rachel E. O'Brien [a], Alexander Laskin [b,*], Julia Laskin [c], Shang Liu [d], Robin Weber [e], Lynn M. Russell [d], Allen H. Goldstein [e,f,**]

[a] Department of Chemistry, University of California, Berkeley, CA, USA
[b] William R. Wiley Environmental and Molecular Sciences Laboratory, Pacific Northwest National Laboratory, Richland, WA 99352, USA
[c] Chemical and Materials Sciences Division, Pacific Northwest National, Laboratory, WA 99352, USA
[d] Scripps Institution of Oceanography, University of California, San Diego, La Jolla, CA, USA
[e] Department of Environmental Science, Policy, & Management, University of California, Berkeley, CA 94720, USA
[f] Department of Civil and Environmental Engineering, University of California, Berkeley, CA 94720, USA

HIGHLIGHTS

- ► We characterize the chemical composition of aerosols collected during CalNex 2010.
- ► We observe changes in the composition of the oligomeric fraction throughout the day.
- ► There were increased numbers of nitrogen-containing compounds at night.
- ► Reactions with ammonia to form imines are possible formation pathways.
- ► Increased numbers of CHO compounds during the day, likely a result of photochemistry.

GRAPHICAL ABSTRACT
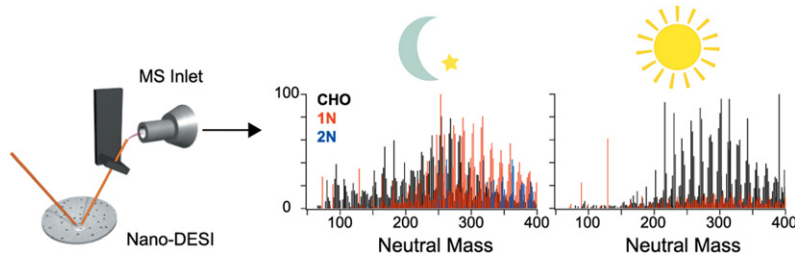
ARTICLE INFO

ABSTRACT

Aerosol samples from the CalNex 2010 field study were analyzed using high-resolution mass spectrometry (HR-MS) coupled to a nanospray desorption/electrospray ionization (nano-DESI) source. The samples were collected in Bakersfield, CA on June 22-23, 2010. The chemical formulas of over 850 unique molecular species were detected in the mass range of 50–400 m/z using positive mode ESI of aerosol samples in the 0.18–0.32 μm size range. Our analysis focused on identification of two main groups: compounds containing only carbon, hydrogen, and oxygen (CHO), and nitrogen-containing organic compounds (NOC). The NOC accounted for 40% (by number) of the compounds observed in the afternoon, and for 52% in the early morning samples. By comparing plausible reactant–product pairs, we propose that over 50% of the NOC in each sample could have been formed through reactions transforming carbonyls into imines. The CHO only compounds were dominant in the afternoon suggesting a photochemical source. The average O/C ratios of all observed compounds were fairly consistent throughout the day, ranging from 0.33 in the morning to 0.37 at night. We conclude that both photooxidation and ammonia chemistry may play a role in forming the compounds observed in this mixed urban-rural environment.

© 2012 Elsevier Ltd. All rights reserved.

 * Corresponding author. P.O. Box 999, K8-88 Richland, WA 99352 USA. Tel.: +1 509 371 6129; fax: +509 371 6039.
 ** Corresponding author. 137 Mulford Hall, Berkeley, CA 94720-3114. Tel.: +1 510 643 2451; fax: +510 643 5098.
   E-mail addresses: Alexander.Laskin@pnl.gov (A. Laskin), ahg@berkeley.edu (A.H. Goldstein).

1. Introduction

Organic compounds have been measured as the dominant fraction of sub-micron aerosols throughout the world (Kanakidou et al., 2005; Fuzzi et al., 2006; Zhang et al., 2007) with multiple studies showing secondary organic aerosol (SOA) as the most abundant portion of total organic aerosol (Turpin and Huntzicker, 1995; Kanakidou et al., 2005). SOA is formed in the atmosphere through gas-to-particle condensation of the oxidation products of volatile organic compounds (VOCs), by heterogeneous gas–particle interactions, and by particle phase reactions (Seinfeld and Pankow, 2003; Ervens et al., 2011). Thousands of primary organic compounds are present in the atmosphere, and the complexity of the organics is increased further by oxidation (Goldstein and Galbally, 2007). The effect that atmospheric aerosols have on the climate by absorbing and scattering radiation, as well as by influencing the lifetime and albedo of clouds, is a major uncertainty in climate modeling (IPCC, 2007). Tying the composition to the properties of the aerosol is inherently obscured by the complexity of the organic constituents. Molecular characterization of organic aerosol is an important step for improving our understanding of aerosol sources, transformations, and their environmental impact (Nizkorodov et al., 2011).

Traditional methods of OA analysis such as gas chromatography–mass spectrometry (GC–MS) are well-suited for identification of many organic molecules, but typically can only identify 10–30% of the OA mass (Rogge et al., 1993). Large (high molecular weight) and polar molecules are generally not measurable by GC. These high molecular weight compounds are often oligomeric, and are sometimes referred to as humic like substances (HULIS) due to their similarities with aqueous and terrestrial humic and fulvic acids (Graber and Rudich, 2006). Oligomeric organics may have a large effect on aerosol properties such as cloud nucleation and light absorption (Graber and Rudich, 2006), yet fundamental understanding of their chemical composition is incomplete. A soft ionization technique such as electrospray ionization (ESI) (Fenn et al., 1990) coupled to mass spectrometry is particularly well suited for the analysis of large polar compounds in complex samples. High-resolution mass spectrometry techniques such as Fourier transform ion cyclotron resonance mass spectrometry (FT-ICR MS) (Kalberer et al., 2004; Tolocka et al., 2004; Reemtsma et al., 2006; Altieri et al., 2008; Mazzoleni et al., 2010; Schmitt-Kopplin et al., 2010) and Orbitrap MS (Laskin et al., 2010; Nguyen et al., 2010) have been successfully used to identify the molecular composition of thousands of organic compounds. Insights into the sources and transformations of aerosols can be gained from changes observed in the chemical composition of ambient samples throughout the day. For example, using an Orbitrap MS, Roach et al. (2010a) observed changes in the chemical composition of ambient aerosols between early morning and mid-day in samples in Mexico City.

The addition of heteroatoms such as nitrogen through gasphase, heterogeneous gas-particle, and condensed-phase chemical reactions adds another level of complexity to the molecular composition of OA (Cape et al., 2011). Nitrogen-containing organic compounds (NOC) have been found to make up 10–20% of the particle mass (Zhang et al., 2002; Holzinger et al., 2010). They can be broadly separated into groups containing either oxidized or reduced nitrogen functional groups. Organonitrates, containing oxidized nitrogen, have been observed in both chamber studies (Fry et al., 2011; Nguyen et al., 2011) and ambient samples (Day et al., 2010; Zaveri et al., 2010). Proposed mechanisms of organonitrate formation include reactions of NO with organic peroxy radicals during the day and reactions of alkenes with NO₃ radicals at night (Ng et al., 2008; Matsunaga and Ziemann, 2009). NOC constituents of OA with reduced nitrogen groups have also been observed in

chamber studies (Laskin et al., 2010) and in field-collected aerosol samples (Pratt et al., 2009; Wang et al., 2010). These compounds can be either primary emissions or products of reactions of, for example, ammonia and amines with carbonyl groups via imine formation reactions (Laskin et al., 2010) and Mannich reactions (Wang et al., 2010). Recently, the use of high-resolution mass spectrometry to characterize the chemical composition of aerosol samples has revealed the presence of a large range of NOC found in atmospheric aerosols (Reemtsma et al., 2006; Schmitt-Kopplin et al., 2010), rainwater (Altieri et al., 2009), and fog water (Mazzoleni et al., 2010). Given the complexity of possible sources and reactions, changes in atmospheric conditions should impact the chemical composition of NOC. Measurements with temporal resolution that separates different times of day should provide valuable insight into the sources and chemical transformations of these compounds.

In typical ESI studies, the aerosol is first extracted into organic solvent and then electrosprayed into the mass spectrometer inlet. Previous studies have shown that chemical modifications of organic compounds such as the acid catalyzed loss of reduced NOC can occur during storage in solvent (Laskin et al., 2010). In principal, the potential alteration of compounds due to reactions in solvent can be reduced by dissolving and ionizing the sample simultaneously, directly from the substrate. A novel method for this type of ambient ionization is nano-desorption/electrospray ionization (nano-DESI) mass spectrometry (Roach et al., 2010b). Roach et al. (2010a) have demonstrated the utility of nano-DESI for soft ionization of organic compounds with no sample preparation and the preservation of some labile species.

In this study we report the chemical composition of organic aerosols collected in Bakersfield, CA, during the CalNex 2010 campaign. Using nano-DESI and high-resolution mass spectrometry we measured the chemical composition of the OA samples. Our analysis focused on two classes of compounds: molecules that contain reduced and oxidized nitrogen and molecules that contain only carbon, hydrogen and oxygen. We report diurnal changes in chemical composition, their relationship to meteorological observations, and show that many of the observed compounds formed through photochemistry and ozonolysis were found predominantly in the afternoon samples.

2. Experimental section

A description of the field site, the meteorology, the ambient sampling methodology, and data analysis are provided in the appendix. Briefly, four samples per day were collected starting at midnight in Bakersfield (35.35°N, 118.97°W) during the CalNex 2010 campaign (NOAA, 2008). The days of June 22nd and 23rd were chosen for in-depth analysis because concurrent measurements indicated high OA loadings. The meteorology on those days was typical for the campaign with higher ozone levels during the day and higher relative humidity during the night (Figure A1). All times discussed here are in local time (PDT). Samples were collected on aluminum foil substrates using a Micro-Orifice Uniform Deposit Impactor (MOUDI) model 100R (MSP, Inc.) without rotation. Samples on the eighth stage of the MOUDI, (aerodynamic diameter of 0.18–0.32 μm), had the highest number of the compounds of interest so samples from this stage were chosen for intensive study. On-line composition of non-refractory components, including the elemental composition of the organic mass (Aiken et al., 2007), was measured using an Aerodyne High-Resolution Time-of-Flight Aerosol Mass Spectrometer (HR-ToF-AMS) at an adjacent trailer (Ahlm et al., 2012). The organic mass in particles with aerodynamic diameters of 0.18–0.32 μm account for 36% of the PM$_{2.5}$ organic mass (Figure A2).

Samples were analyzed at Environmental Molecular Science Laboratory located in Richland, WA. Analysis was performed with an LTQ/Orbitrap mass spectrometer (Thermo Electron, Bremen, Germany) equipped with a nano-DESI source (Roach et al., 2010a,b). The source is assembled from two fused-silica capillaries (193 μm o.d./50 μm i.d, Polymicro Technologies LLC, Phoenix, AZ). The primary capillary supplies the solvent, acetonitrile, and maintains a small droplet of solvent over the analyte area. The analyte molecules that dissolved into the solvent are transferred into the mass spectrometer inlet through the nano-spray capillary. A voltage of $\sim \pm 6$ kV was applied between the capillary end and the mass spectrometer inlet to obtain stable spray of charged droplets. The solvent was supplied at 1.5–2.5 μL min^{-1} flow rate to maintain a stable droplet on the surface. Thus, this is an analysis of the compounds that are dissolved in acetonitrile and ionized with these spray conditions. The system was operated in the positive and negative ion modes with a resolution of 60,000 m/Δm at 400 m/z. For each mass spectrum approximately 50 individual scans were averaged. The majority of the data discussed hereafter were obtained in the positive ion mode, only the elemental ratios from negative mode ESI are discussed; a full analysis of the negative ion mode will be presented in a future publication. The instrument was mass calibrated using a standard ESI calibration mix of caffeine, MRFA, and Ultramark 1621.

Time-dependent MS signal was acquired for each of the samples, where the acquisition was started first for ∼1 min on the substrate outside of the sample deposition area (background MS). Then, the substrate was moved such that the probe was positioned over the sample containing area while data acquisition was continued for an additional 2–3 min (sample MS). Mass spectral features with a signal-to-noise ratio of at least 3 were extracted from background and sample raw spectra using the Decon2LS program developed at PNNL (http://ncrr.pnl.gov/software/). Peaks recorded in the sample MS spectrum were eliminated from the sample peak list if the intensity in the sample MS was less than ten times the intensity in the background MS. An Excel macro was used for the background subtraction and to remove compounds with ^{13}C isotopes. The remaining peaks were assigned molecular formulas using Formula Calculator v. 1.1 developed at the National High Magnetic Field Laboratory (http://magnet.fsu.edu/∼midas/download.html). The molecular formula search was performed using the following parameters: $C_{0-100}H_{0-200}O_{0-50}N_{0-3}S_{0-1}Na_{0-1}^{+}$. Approximately 80–90% of the peaks could be assigned molecular formulas. Assignments were aided by Kendrick analysis (Kendrick, 1963) using O and $C_3H_4O_2$ as bases, and a second-order mass defect analysis using a sequence of CH_2 and H_2 bases (Roach et al., 2011). A mass range of 50–1000 m/z was collected for each sample; however, we limit our discussion to the mass range of 50–400 Da because we can unambiguously assign identities give the mass accuracy and resolution used in this study. Further discussion on the Kendrick analysis and the assignments of molecular formulas is provided in the appendix.

All assigned peaks have a mass error within ±2 ppm. Between 30 and 70% of the peaks in these samples have exact masses with potential assignments of either $C_xH_yO_zNa^+$ or $C_{x-3}H_{y-2}N_2O_{z+2}H^+$ and $C_xH_yNO_zNa^+$ or $C_{x-3}H_{y-2}N_3O_{z+2}H^+$. Peaks with these possible assignments that had only one option within ±2 ppm were kept while those that had both options within ±2 ppm were removed from the peak list. This removed less than 0.1% of the peaks in each sample. The mass spectra have been separated by the number of nitrogen atoms in the chemical formula. Data representing compounds containing no nitrogen atoms will be referred to as CHO. Data for compounds containing one or two nitrogen atoms will be referred to as 1N or 2N respectively. For the comparison of

the positive and negative mode NOC the data will be referred to as NOC$^+$ and NOC$^-$ and the NOC$^-$ contains no sulfur.

Inorganic ions such as sodium, potassium, magnesium, etc. can be present in ambient samples and can affect the ionization efficiency and form adducted complexes. From analysis of the exact masses and isotope distributions, no multiply charged ions and no complexes with potassium ions were observed. The possibility of ammonium complexes is discussed in detail below. Other potentially complicating factors include the formation of noncovalently bound clusters of smaller organic molecules and the in-source fragmentation of larger organic molecules. Compounds present in the samples were observed as either protonated or sodiated molecules in the positive mode spectra, and as deprotonated molecules in the negative mode spectra. The compounds were converted to neutral species by subtracting either the exact mass of a proton or a sodium ion from [M+H]$^+$ or [M+Na]$^+$ respectively or by adding the mass of a proton to [M+H]$^-$. Approximately 2–18% of the peaks in each sample were detected as both a sodiated and protonated compound in the positive mode spectra. For these peaks, the sum of the intensities was used and the duplicate peaks were merged so that all the peaks shown in the figures and considered in the data analysis are unique.

3. Results and discussion

3.1. Mass spectra and elemental composition

High-resolution positive-mode nano-DESI mass spectra for the four samples collected on June 23, 2010 in Bakersfield, CA are shown in Fig. 1. The molecular formulas of approximately 700–800 compounds were identified in each mass spectrum between 50 and 400 Da. With electrospray ionization, the measured peak intensities are affected by the solution composition, the concentration, and the ionization efficiency of the sample molecules. Thus, the intensities do not directly correlate to the absolute concentrations in the sample. However, qualitative information on the relative concentrations of molecules between samples can still be obtained. The groups of peaks in the figure have been separated by the number of nitrogen atoms in their chemical formulas. Data plotted for CHO only compounds are colored black and data for 1N and 2N compounds are colored red and blue respectively. A very small number of compounds with one sulfur atom or three nitrogen atoms were measured. All of those compounds were below 15% relative intensity and are not shown in Fig. 1, but are listed in Table A1. In ambient samples, sulfur-containing compounds are typically observed in negative mode ESI with many fewer observed in positive mode ESI (Mazzoleni et al., 2010; Lin et al., 2012). The pie charts represent the percentage of detected species that fall into each category. Since individual species could have many different isomeric structures, the percentages reflect only the number of unique molecular formulas and do not reflect the number of unique molecules in each category.

The intensity distributions and the number of compounds in each group changed throughout the day. The percent of NOC species, including those containing two nitrogen atoms, was largest between midnight and 6 am (Fig. 1a). From 6 am to noon (Fig. 1b), the number of NOC species decreased slightly and the number of CHO species increased. An increase in both the percentage of and the relative intensities of the CHO species occurred in the noon to 6 pm sample (Fig. 1c) when the number and relative intensities of NOC reached their lowest values. This trend reversed in the 6 pm to midnight sample (Fig. 1d) when the percentage and relative intensity of the NOC species increased. Similar patterns were observed for the samples collected on June 22nd (Figure A3). In this
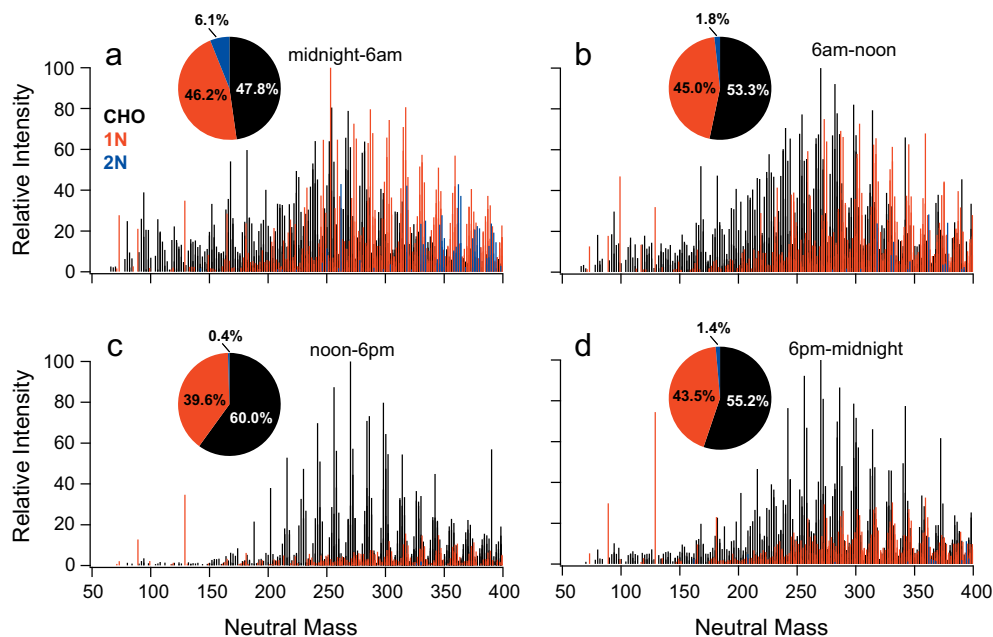
Fig. 1. Reconstructed mass spectra of the identified peaks in each of the four samples collected on June 23rd. The pie charts show the percentage of compounds by number that fall in each group.

study, eight samples over 2 days were analyzed and, thus, statistical analysis of the observed trends is not presented.

A Van Krevelen diagram is presented in Fig. 2 with the H/C ratios plotted against the O/C ratios of the neutral compounds identified in the sample collected on June 23rd from midnight to 6 am. The Van Krevelen plots for the other samples are similar and are shown in Figure A4. This type of diagram provides a comparison of the degree of saturation vs. oxidation of the compounds. The data is broken down by the number of nitrogen atoms in the compound following the color scheme used in Fig. 1. Each point on the diagram can represent more than one molecule since multiple compounds can have the same combination of H/C and O/C ratios. The range of values plotted in the diagrams does not change significantly throughout the day for most of the CHO compounds (Figure A4). The average elemental ratios, e.g. <O/C>, discussed below are weighted by the relative intensities in the mass spectra (Nguyen et al., 2010). The <H/C> value of all of the samples was 1.6 and the <O/C> values ranged between 0.33 in the samples from midnight to noon to 0.37 in the 6 pm–midnight sample. Aerosol Mass Spectrometers (AMS) measure the composition of the aerosol in real time and the <O/C> and <H/C> values can be compared
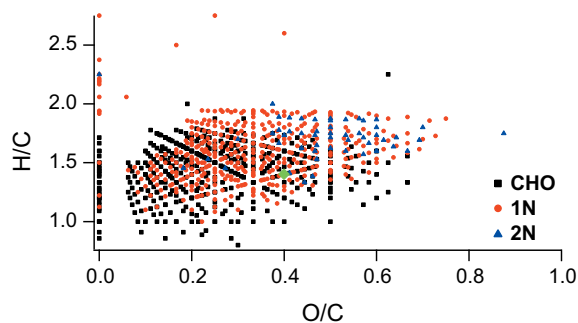
between the two techniques (Baer et al., 2006). Comparing these values to AMS data must be done with caution, however, because of a bias toward more sensitive detection of more oxidized compounds that are preferentially found in negative mode ESI which leads to higher <O/C> values in negative mode data. Additionally, the aerosol size fraction for this analysis was 0.18–0.32 μm and AMS was sampling up to 1.0 μm. However, no dependence of the <O/C> on the aerosol size was found from an analysis of the AMS data. For the four samples on June 23rd, the <O/C> values of 0.33–0.36 for the positive mode data and 0.57–0.71 for the negative mode data bracket the <O/C> values of 0.40–0.48 measured with the AMS in Bakersfield on the same day (Table A2). The <O/C> values obtained in this study also compare favorably with AMS data collected in Riverside during the SOAR-1 campaign and the <O/C> measurements from the AMAZE-08 campaign in the Amazon basin (Heald et al., 2010). Our data also compare well to the averaged AMS data and the nano-DESI data from the MILAGRO campaign that have <O/C> values of 0.42–0.47 and 0.37 respectively (Roach et al., 2010a).

In Fig. 2 and Figure A3, the majority of points from the NOC are shown to occur in the same O/C vs. H/C region as the CHO points. The intensity weighted <N/C> values for the positive mode ESI data on June 23rd ranged from 0.012 in the noon to 6 pm sample to 0.041 in the midnight to 6 am sample. These values are 3–10 times higher than the average N/C values measured with AMS in Bakersfield. The best comparisons were in the afternoon and evening samples (Table A2). The high ionization efficiency of reduced nitrogen-containing compounds with ESI (Oss et al., 2010) could be one reason for these differences. More work comparing the responses of the two different techniques to nitrogen-containing compounds is necessary to fully explain these results.

3.2. CHO compounds

Ozone concentration during sample collection was high in the afternoon and low at night (Figure A1). On June 23rd the highest levels of ozone occurred from noon to 6 pm with an 8 h average of 85 ppb and a peak of 92 ppb at 1:30 pm, exceeding the regulatory

Fig. 2. Van Krevelen diagram for the sample collected on June 23rd midnight to 6 am. Black markers are CHO only and red and blue correspond to compounds with one and two nitrogen atoms respectively. The large diamond (0.4, 1.4) corresponds to AMS data averaged over the same sample time. (For interpretation of the references to color in this figure legend, the reader is referred to the web version of this article.)
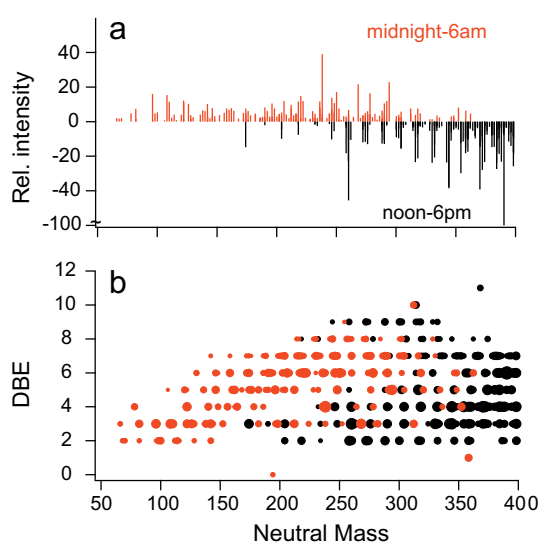
standard set by the California Air Resources Board of 70 ppb ozone over 8 h (CARB, 2012). The high ozone levels correlated with appearance of the predominant CHO compounds in the mass spectra from noon to 6 pm suggesting that these compounds were secondary products of day time oxidation including ozonolysis and/or photochemical reactions. Fig. 3a shows a comparison between the midnight–6 am and the noon–6 pm samples of the CHO peaks that were unique to each sample. The double-bond equivalence (DBE) values shown in Fig. 3b were calculated from the chemical formulas of the neutral compounds using Eq. (1):

$$DBE = 1 + c - h/2 \tag{1}$$

where c and h refer to the number of carbon and hydrogen atoms in the chemical formula. The DBE represents the sum of all rings and double bonds in the molecule. The midnight to 6am sample had 165 unique compounds with a median neutral mass of 214 Da and the noon to 6 pm sample had 160 unique compounds with a median neutral mass 333 Da. The DBE values ranged from about 2 to 9 in both of the samples. Almost all of the low-mass compounds (<200 Da) were unique to the midnight to 6 am sample. These compounds could be either local emissions or small molecules that do not remain in the aerosol phase during the higher temperatures of mid-day. The higher-mass oligomeric compounds that were unique to the day time sample were likely products relevant to ozonolysis and/or photochemical processes.

3.3. Organic nitrogen

The observed diurnal trend of the NOC fractions in the four samples shown in Fig. 1 likely reflects different processes in the atmospheric chemistry occurring at night and during the day. Both the number and the relative intensities of NOC were largest during the night, indicating that nitrate radical chemistry could have been a significant source of these compounds. It should be noted, however, that since this is positive mode ESI, the ionization of organonitrate compounds will be relatively disfavored unless they contain a group that can solvate the positive charge. Ion

chromatography measurements of the gas-phase concentrations of ammonia showed an average diurnal concentration range for the campaign of ∼700–900 nmol m^{-3} (Markovic et al., unpublished results) which could have been available for reactions that add reduced nitrogen to chemical compounds such as Mannich reactions (Wang et al., 2010) and imine formation reactions (Laskin et al., 2010).

The number of oxygen atoms in the 1N subgroup ranges from zero to ten with approximately 15% of those compounds containing less than three oxygen atoms in the molecular formula. Approximately 70–90% of the 2N compounds, in each sample, had enough oxygen atoms for every nitrogen atom to potentially be in an organonitrate group. However, the O/C range for the positive mode (NOC$^+$) was lower overall than the O/C range for the negative mode (NOC$^-$), where the ionization of organonitrates was favored. Fig. 4 shows a Van Krevelen diagram for the NOC$^+$ and NOC$^-$ data collected from midnight to 6am on June 23rd. Similar Van Krevelen diagrams for the other samples on June 23rd are shown in Figure A5. The lower average O/C range of the positive mode data suggests that a large percentage of the NOC$^+$ contain reduced nitrogen.

In the above discussion, the NOC were assumed to be covalently bound. To investigate the possible formation of [M+NH$_4^+$] compounds, in source fragmentation was performed by applying an accelerating voltage in the ion optics which should dissociate noncovalent complexes formed in electrospray (Duffin et al., 1991). A complete analysis requires knowledge of the structure of the molecules since that determines how tightly the ammonium may be adducted and thus, what voltages are necessary to break non-covalent clusters. Covalently bound nitrogen molecules may also fragment under these conditions. Future work should involve MS/MS on the isolated compounds to determine structures of both the CHO only compounds and the NOC. The NOC that disappeared as a result of collision-induced dissociation (CID) in a 30 V field gradient were analyzed using three criteria to determine which of these compounds were more likely to be ammonium adducts. Compounds that were below 5% relative intensity were removed from the list because the natural variability of the peak intensities precludes them being used in this type of analysis. NOC with sodium as the charge carrier were removed from the list since all of the molecules were singly charged and thus could not have simultaneous adduction of both sodium and ammonium ions. Finally, compounds that were observed in the negative mode were also removed since negatively charged ions with ammonium adducts are unlikely. For this to be the case the ammonium would have to be solvated by a negative charge, however based on the thermodynamics of the protonation of a carboxylate group and the proton affinity of ammonia in the gas-phase, a carboxylate group would readily abstract a proton from an ammonium adduct leaving
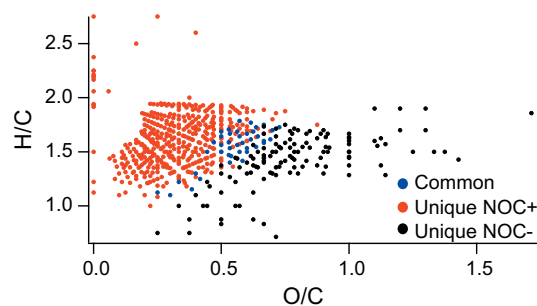

Fig. 3. Comparison of CHO peaks that are unique between midnight to 6 am (red) and noon to 6 pm (black). (a) Mass spectra of the unique peaks are shown as positive and negative signal to aid in the comparison. (b) DBE versus the neutral mass of the unique peaks is shown. The size of the points is proportional to the logarithm of the relative peak intensity. (For interpretation of the references to color in this figure legend, the reader is referred to the web version of this article.)

Fig. 4. Van Krevelen diagram for NOC from the sample collected on June 23rd from midnight to 6 am. Blue markers are compounds measured in both negative and positive mode, red and black are compounds measured in only the positive and negative mode respectively. (For interpretation of the references to colour in this figure legend, the reader is referred to the web version of this article.)

Table 1
Number of occurrences of NOC$^+$, per sample, that have mass shifts corresponding to the formation of products by reactions r1–r3.

| Sample	Total NOC	Number of occurrences			
		r1 +NH; −O	r2 +N; −H; −O$_2$	r3 r2: +2H; −2H	Total number of unique occurrences
6/22 midnight–6 am	375	183	138	130	242
6/22 6 am–noon	407	146	104	106	200
6/22 noon–6 pm	326	205	149	146	251
6/22 6 pm–midnight	387	231	180	188	285
6/23 midnight–6 am	456	234	155	158	270
6/23 6 am–noon	398	220	159	172	269
6/23 noon–6 pm	277	190	151	118	223
6/23 6 pm–midnight	361	235	186	194	290

the neutral ammonia to evaporate (Table A3). The remaining NOC made up 0.5–5% of the total number of NOC in each sample. Only 32 compounds failed the tests and were unique to one sample and only seven failed the tests in more than one sample (Table A4). This suggests that the amount of ammonium adduction was likely very small.

3.4. Formation of nitrogen-containing organic compounds

The addition of reduced nitrogen to organic molecules can occur via imine formation reactions where carbonyl oxygen atoms are replaced by NH groups. The following reaction was reported in laboratory studies of SOA aging through heterogeneous uptake and reaction of gaseous ammonia with wet SOA particles (r1) (Laskin et al., 2010).
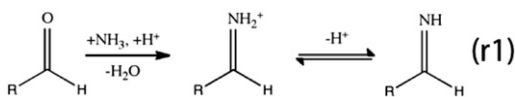
Products of the above reaction were found to undergo additional cyclization and disproportionation reactions in the condensed aqueous phase of SOA (r2 and r3) (Laskin et al., 2010).
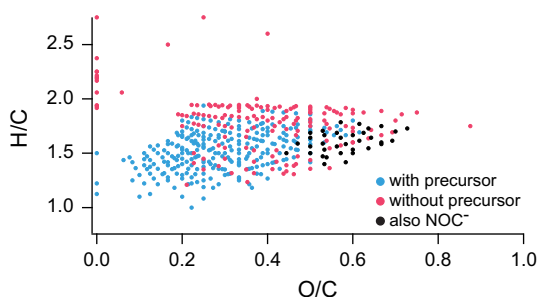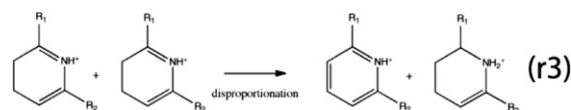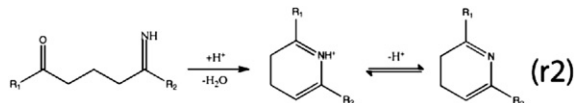
Fig. 5. Van Krevelen diagram for NOC from the sample collected on June 23rd from midnight to 6 am. the light blue points correspond to compounds that had a precursor with the mass differences given by reactions r1, r2, or r3. The pink dots are compounds for which we do not observe a precursor and the black dots are compounds without an observed precursor that are also measured in the negative mode. (For interpretation of the references to colour in this figure legend, the reader is referred to the web version of this article.)

The 2N compounds could be formed through subsequent reactions of carbonyl groups on newly formed imines (Laskin et al., 2010). The potential prevalence of these reactions in forming the observed NOC was analyzed using the mass differences between the reactants and products in reactions r1–r3 to find possible precursor–product pairs in the mass spectra. Table 1 shows a summary of the number of NOC that had mass differences from reactions r1–r3 relating potential precursor–product pairs. The "total number of unique occurrences" shows the full number of NOC that can be explained by these reactions; note that there is a great deal of overlap between the three reactions. The total number of compounds that have corresponding precursors for these samples was on the same order of magnitude as results from chemically aged SOA (Laskin et al., 2010), and approximately 50–80% of the identified NOC could potentially be explained by this type of chemistry. A large part of the variability in the total coverage was likely driven by the presence or lack of potential precursors since the number of CHO compounds observed changed throughout the day.

Fig. 5 shows a Van Krevelen diagram for the NOC compounds for the midnight to 6am sample on June 23rd. The light blue points were compounds found to have precursors in the sample that correspond to reactions r1–r3, while the pink points were compounds that had no corresponding precursors. The black points were compounds with no corresponding precursor that were also observed in the negative mode. The compounds observed in the negative mode were all located at relatively high O/C ratios consistent with organonitrates. The NOC that do not have a precursor were predominantly located in the upper H/C range and are likely either local emissions, compounds where the precursor was depleted below the limit of detection, or they could be formed through other reactions such as Mannich reactions with small aldehydes (Wang et al., 2010). The oxidation state of nitrogen is not evident from a given chemical formula and there are many potential sources and formation mechanisms for the observed NOC. Additionally, presence of precursor–product pairs is not definitive proof of a reaction pathway; future work with MS/MS analysis to gain structural information is necessary to fully characterize formation mechanisms. We present these reactions as possible mechanisms for the formation of compounds containing reduced nitrogen groups and conclude that it is likely ammonia plays a role in the chemistry of the organic fraction in Bakersfield.

4. Summary

The molecular composition of size-resolved aerosol samples collected in Bakersfield California during CalNex 2010 was investigated using nano-DESI and high-resolution mass spectrometry. Positive mode ESI was used and three groups of compounds were observed: compounds containing only carbon, hydrogen, and

oxygen (CHO) and compounds containing one or two nitrogen atoms (NOC). Changes in the chemical composition were observed throughout the day with more NOC identified in the night samples and more CHO only compounds identified during the day. The high number of CHO compounds coincided with high ozone and high photoactive radiation levels consistent with photochemistry/ozonolysis as major sources. The NOC had lower O/C values than the NOC measured using negative mode ESI and thus likely contained reduced nitrogen groups. Over 50% of the NOC had precursor–product pairs consistent with imidization and cyclization reactions. These reactions involve ammonia and carbonyl groups on the precursor indicating the potential role of ammonia in forming NOC. Detailed analysis of the changes in the chemical composition throughout the day have elucidated the roles of nitrogen, photochemistry, and particle phase reactions on the formation and transformation of high molecular weight oligomers in Bakersfield California.

Acknowledgments

Appendix A. Supplementary data

Supplementary data related to this article can be found at http://dx.doi.org/10.1016/j.atmosenv.2012.11.056.

References

Ahlm, L., et al., 2012. Formation and growth of ultrafine particles from secondary sources in Bakersfield, California. Journal of Geophysical Research-Atmospheres 117 (D00V08). http://dx.doi.org/10.1029/2011JD017144.

Aiken, A.C., et al., 2007. Elemental analysis of organic species with electron ionization high-resolution mass spectrometry. Analytical Chemistry 79 (21), 8350–8358.

Altieri, K.E., et al., 2008. Oligomers formed through in-cloud methylglyoxal reactions: chemical composition, properties, and mechanisms investigated by ultrahigh resolution FT-ICR mass spectrometry. Atmospheric Environment 42 (7), 1476–1490.

Altieri, K.E., et al., 2009. Oligomers, organosulfates, and nitrooxy organosulfates in rainwater identified by ultra-high resolution electrospray ionization FT-ICR mass spectrometry. Atmospheric Chemistry and Physics 9 (7), 2533–2542.

Baer, T., et al., 2006. Aerosol mass spectrometry: an introductory review. International Journal of Mass Spectrometry 258 (1–3), 2–12.

Cape, J.N., et al., 2011. Organic nitrogen in the atmosphere — where does it come from? A review of sources and methods. Atmospheric Research 102 (1–2), 30–48.

CARB: California Air Resources Board, 2012. Ambient Air Quality Standards. Available from: http://www.arb.ca.gov/research/aaqs/aaqs2.pdf (accessed 04.07.2012).

Day, D.A., et al., 2010. Organonitrate group concentrations in submicron particles with high nitrate and organic fractions in coastal southern California. Atmospheric Environment 44 (16), 1970–1979.

Duffin, K.L., et al., 1991. Electrospray and tandem mass-spectrometric characterization of acylglycerol mixtures that are dissolved in nonpolar-solvents. Analytical Chemistry 63 (17), 1781–1788.

Ervens, B., et al., 2011. Secondary organic aerosol formation in cloud droplets and aqueous particles (aqSOA): a review of laboratory, field and model studies. Atmospheric Chemistry and Physics 11 (21), 11069–11102.

Fenn, J.B., et al., 1990. Electrospray ionization — principles and practice. Mass Spectrometry Reviews 9 (1), 37–70.

Fry, J.L., et al., 2011. SOA from limonene: role of NO_3 in its generation and degradation. Atmospheric Chemistry and Physics 11 (8), 3879–3894.

Fuzzi, S., et al., 2006. Critical assessment of the current state of scientific knowledge, terminology, and research needs concerning the role of organic aerosols in the atmosphere, climate, and global change. Atmospheric Chemistry and Physics, 62017–62038.

Goldstein, A.H., Galbally, I.E., 2007. Known and unexplored organic constituents in the earth's atmosphere. Environmental Science & Technology 41 (5), 1514–1521.

Graber, E.R., Rudich, Y., 2006. Atmospheric HULIS: how humic-like are they? A comprehensive and critical review. Atmospheric Chemistry and Physics, 6729–6753.

Heald, C.L., et al., 2010. A simplified description of the evolution of organic aerosol composition in the atmosphere. Geophysical Research Letters 37 (L08803). http://dx.doi.org/10.1029/2010gl042737.

Holzinger, R., et al., 2010. Analysis of the chemical composition of organic aerosol at the Mt. Sonnblick observatory using a novel high mass resolution thermal-desorption proton-transfer-reaction mass-spectrometer (hr-TD-PTR-MS). Atmospheric Chemistry and Physics 10 (20), 10111–10128.

IPCC, 2007. In: Solomon, S., Qin, D., Manning, M., Chen, Z., Marquis, M., Averyt, K.B., Tignor, M., Miller, H.L. (Eds.), Climate Change 2007: the Physical Science Basis. Contribution of Working Group I to the Fourth Assessment Report of the Intergovernmental Panel on Climate Change. Cambridge University Press, Cambridge, UK and New York, NY, USA.

Kalberer, M., et al., 2004. Identification of polymers as major components of atmospheric organic aerosols. Science 303 (5664), 1659–1662.

Kanakidou, M., et al., 2005. Organic aerosol and global climate modelling: a review. Atmospheric Chemistry and Physics, 51053–51123.

Kendrick, E., 1963. A mass scale based on Ch2=14.0000 for high resolution mass spectrometry of organic compounds. Analytical Chemistry 35 (13), 2146.

Lin, P., et al., 2012. Elemental composition of HULIS in the Pearl River delta region, China: results inferred from positive and negative electrospray high resolution mass spectrometric data. Environmental Science & Technology 46 (14), 7454–7462.

Laskin, J., et al., 2010. High-resolution desorption electrospray ionization mass spectrometry for chemical characterization of organic aerosols. Analytical Chemistry 82 (5), 2048–2058.

Markovic, M.Z., et al., unpublished results. Measurements and modeling of the water-soluble composition of PM2.5 and associated precursor gases in Bakersfield, CA during CalNex 2010.

Matsunaga, A., Ziemann, P.J., 2009. Yields of beta-hydroxynitrates and dihydroxynitrates in aerosol formed from OH radical-initiated reactions of linear alkenes in the presence of NO(x). Journal of Physical Chemistry A 113 (3), 599–606.

Mazzoleni, L.R., et al., 2010. Water-soluble atmospheric organic matter in fog: exact masses and chemical formula identification by ultrahigh-resolution Fourier transform ion cyclotron resonance mass spectrometry. Environmental Science & Technology 44 (10), 3690–3697.

Ng, N.L., et al., 2008. Secondary organic aerosol (SOA) formation from reaction of isoprene with nitrate radicals (NO(3)). Atmospheric Chemistry and Physics 8 (14), 4117–4140.

Nguyen, T.B., et al., 2010. High-resolution mass spectrometry analysis of secondary organic aerosol generated by ozonolysis of isoprene. Atmospheric Environment 44 (8), 1032–1042.

Nguyen, T.B., et al., 2011. Nitrogen-containing organic compounds and oligomers in secondary organic aerosol formed by photooxidation of isoprene. Environmental Science & Technology 45 (16), 6908–6918.

Nizkorodov, S.A., et al., 2011. Molecular chemistry of organic aerosols through the application of high resolution mass spectrometry. Physical Chemistry Chemical Physics 13 (9), 3612–3629.

NOAA: National Oceanic and Atmospheric Administration, 2008. 2010 CalNex White Paper: Research at the Nexus of Air Quality and Climate Change. Available from: http://www.esrl.noaa.gov/csd/projects/calnex/whitepaper.pdf (accessed 23.07.2012).

Oss, M., et al., 2010. Electrospray ionization efficiency scale of organic compounds. Analytical Chemistry 82 (7), 2865–2872.

Pratt, K.A., et al., 2009. Seasonal volatility dependence of ambient particle phase amines. Environmental Science & Technology 43 (14), 5276–5281.

Reemtsma, T., et al., 2006. Identification of fulvic acids and sulfated and nitrated analogues in atmospheric aerosol by electrospray ionization Fourier transform ion cyclotron resonance mass spectrometry. Analytical Chemistry 78 (24), 8299–8304.

Roach, P.J., et al., 2010a. Molecular characterization of organic aerosols using nanospray-desorption/electrospray ionization-mass spectrometry. Analytical Chemistry 82 (19), 7979–7986.

Roach, P.J., et al., 2010b. Nanospray desorption electrospray ionization: an ambient method for liquid-extraction surface sampling in mass spectrometry. Analyst 135 (9), 2233–2236.

Roach, P.J., et al., 2011. Higher-order mass defect analysis for mass spectra of complex organic mixtures. Analytical Chemistry 83 (12), 4924–4929.

Rogge, W.F., et al., 1993. Quantification of urban organic aerosols at a molecular-level – identification, abundance and seasonal-variation. Atmospheric Environment Part A-General Topics 27 (8), 1309–1330.

Schmitt-Kopplin, P., et al., 2010. Analysis of the unresolved organic fraction in atmospheric aerosols with ultrahigh-resolution mass spectrometry and nuclear magnetic resonance spectroscopy: organosulfates as photochemical smog constituents. Analytical Chemistry 82 (19), 8017–8026.

Seinfeld, J.H., Pankow, J.F., 2003. Organic atmospheric particulate material. Annual Review of Physical Chemistry, 54121–54140.

Tolocka, M.P., et al., 2004. Formation of oligomers in secondary organic aerosol. Environmental Science & Technology 38 (5), 1428–1434.

Turpin, B.J., Huntzicker, J.J., 1995. Identification of secondary organic aerosol episodes and quantitation of primary and secondary organic aerosol concentrations during SCAQS. Atmospheric Environment 29 (23), 3527–3544.

Wang, X.F., et al., 2010. Evidence for high molecular weight nitrogen-containing organic salts in urban aerosols. Environmental Science & Technology 44 (12), 4441–4446.

Zaveri, R.A., et al., 2010. Nighttime chemical evolution of aerosol and trace gases in a power plant plume: implications for secondary organic nitrate and organo-sulfate aerosol formation, NO(3) radical chemistry, and N(2)O(5) heterogeneous hydrolysis. Journal of Geophysical Research-atmospheres 115 (D12304). http://dx.doi.org/10.1029/2009JD013250.

Zhang, Q., et al., 2002. Water-soluble organic nitrogen in atmospheric fine particles (PM2.5) from northern California. Journal of Geophysical Research-atmospheres 107 (D11), 4112. http://dx.doi.org/10.1029/2001jd000870.

Zhang, Q., et al., 2007. Ubiquity and dominance of oxygenated species in organic aerosols in anthropogenically-influenced Northern Hemisphere midlatitudes. Geophysical Research Letters 34 (13), L13801. http://dx.doi.org/10.1029/2007GL029979.